

New physics in top production

G. SERVANT

*CERN, Theory division - CH-1211 Genève, Switzerland and
IPhT CEA Saclay - France*

ricevuto l' 1 Marzo 2012

pubblicato online il 5 Giugno 2012

Summary. — In theories that provide a mechanism for mass generation, we expect new physics to have a large coupling to the top quark. It is therefore natural to use top quark observables to test the mechanism responsible for electroweak symmetry breaking. In the first part of this paper, I discuss the production and decay of top partners at the LHC, stressing the theoretical motivations in the context of composite Higgs models. I then present an effective field theory approach to opposite and same sign top quark pair production and discuss the general model-independent constraints that can be obtained at the LHC on the restricted number of dimension-six operators affecting $t\bar{t}$ and tt production.

PACS 14.65.Ha – Top quarks.

1. – The top quark as a link to beyond the Standard Model physics

As of today, there are still two paradigms for electroweak symmetry breaking: weakly coupled new physics at the TeV scale, namely supersymmetry, and strongly coupled new physics, as in Higgsless or composite Higgs models. Particularly well motivated is the case in which the Higgs is a pseudo Goldstone boson of a spontaneously broken global symmetry (a kind of pion from a new strong sector) [1] and the fermion mass spectrum is explained by partial compositeness. In this framework, which has attracted considerable attention in the last few years, the top quark is mostly composite while all other SM fermions are elementary. A generic prediction of this class of model is the existence of light fermionic top partners, comprising at least two $SU(2)_L$ doublets: (T, B) carrying the same quantum numbers as the SM (t_L, b_L) , and the so-called *custodian* more exotic doublet, $(T_{5/3}, T_{2/3})$, where $T_{5/3}$ carries an electric charge $Q_e = 5/3$ [2]. They couple strongly to the third generation SM quarks plus longitudinal W , Z and Higgs. In particular, B and $T_{5/3}$ decay into tW .

Naturalness as well as the latest LHC constraints on the Higgs mass imply that the mass of the top partners should be in the $\sim 500\text{ GeV} - 1.5\text{ TeV}$ range [2-4]. Their

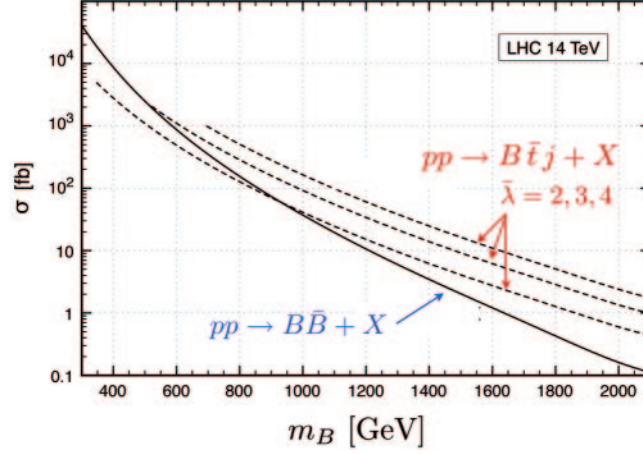


Fig. 1. – Cross section for pair production (solid line) and single production (dotted lines) of fermionic top partners, from [5].

pair and single production cross sections at the LHC are shown in fig. 1. The pair-production of B and $T_{5/3}$ leads to the $t\bar{t}WW$ final state (see fig. 2). It is promising in the same sign dilepton channel [5-7]. LHC constraints using 1.14fb^{-1} of data are $m_B, m_{T_{5/3}} > 495\text{ GeV}$ [8]. The expected reach at 14 TeV is of the order of 1.5 TeV. The LHC will therefore probe the full mass range that is consistent with naturalness considerations.

It has been shown recently in [9,10] that a much higher mass can be reached if the B is singly produced together with a light b via a massive spin-1 gluon G^* , leading to the same final state as $t\bar{t}$. The mass reach on B is less model independent as it requires G^* lighter than $\sim 5\text{ TeV}$ and it depends on specific relations between parameters of the model. This process is nevertheless interesting and should be investigated experimentally. The search for heavy gluon resonances in the $t\bar{t}$ channel is on the other hand actively pursued and was presented at this conference. I will now move to a different discussion, that applies if resonances are too heavy to be accessible at the LHC. In this case, we can follow a low energy effective field theory approach to characterize new physics. Our goal is to propose a general model-independent analysis to study new physics in the $t\bar{t}$ and tt final states.

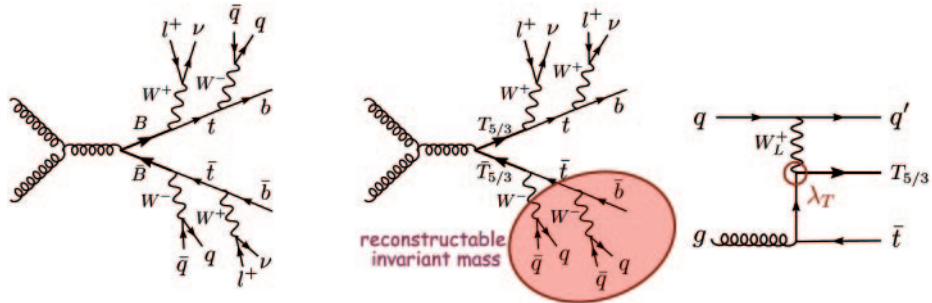


Fig. 2. – Pair production of B and $T_{5/3}$ and single production of $T_{5/3}$.

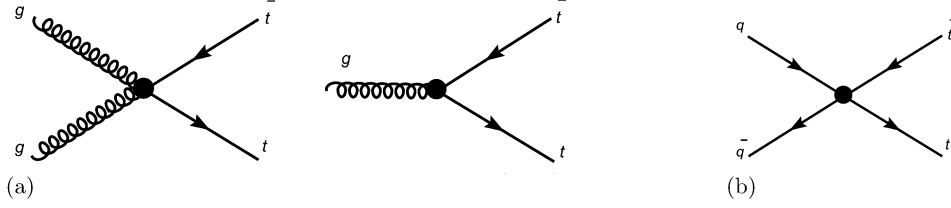


Fig. 3. – Relevant operators for $t\bar{t}$ production at hadron colliders. (a) Chromomagnetic operator $\mathcal{O}_{hg} = (H\bar{Q})\sigma^{\mu\nu}T^A t G_{\mu\nu}^A$. (b) Four-fermion operators.

2. – Effective field theory for opposite sign top quark pair production

We report the work presented in ref. [11] which studies deviations to top quark pair production at hadron colliders coming from dimension-six operators interfering with the SM at tree level. The relevant effective Lagrangian for $t\bar{t}$ production is written as

$$\mathcal{L}_{t\bar{t}} = +\frac{1}{\Lambda^2} \sum_i c_i \mathcal{O}_i.$$

We neglect electroweak corrections and only consider QCD amplitudes. In addition, we focus on *top-philic* new physics, meaning that we ignore interactions that would only affect the gluon vertex. Under these assumptions, there are only 8 relevant independent operators, one being the chromomagnetic dipole moment of the top quark

$$\mathcal{O}_{hg} = [(H\bar{Q})\sigma^{\mu\nu}T^A t] G_{\mu\nu}^A$$

and the others being four-fermion operators with a top and an antitop together with a pair of light quark and antiquark that can be organized following their chiral structures:

$$\begin{aligned} \mathcal{O}_{Qq}^{(8,1)} &= (\bar{Q}\gamma^\mu T^A Q) (\bar{q}\gamma_\mu T^A q), & \mathcal{O}_{Qq}^{(8,3)} &= (\bar{Q}\gamma^\mu T^A \sigma^I Q) (\bar{q}\gamma_\mu T^A \sigma^I q), \\ \mathcal{O}_{tu}^{(8)} &= (\bar{t}\gamma^\mu T^A t) (\bar{u}\gamma_\mu T^A u), & \mathcal{O}_{td}^{(8)} &= (\bar{t}\gamma^\mu T^A t) (\bar{d}\gamma_\mu T^A d), \\ \mathcal{O}_{Qu}^{(8)} &= (\bar{Q}\gamma^\mu T^A Q) (\bar{u}\gamma_\mu T^A u), & \mathcal{O}_{Qd}^{(8)} &= (\bar{Q}\gamma^\mu T^A Q) (\bar{d}\gamma_\mu T^A d), \\ \mathcal{O}_{tq}^{(8)} &= (\bar{q}\gamma^\mu T^A q) (\bar{t}\gamma_\mu T^A t), \end{aligned}$$

where $Q = (t_L, b_L)$ denotes the left-handed weak doublet of the third quark generation, t is the right-handed top quark, T^A are the generators of $SU(3)$, σ^I are the Pauli matrices, q and u and d are respectively the left- and right-handed components of the first two generations. The new vertices are shown in fig. 3.

Interestingly, physical observables such as the $t\bar{t}$ production total cross section, the $m_{t\bar{t}}$ invariant-mass distribution or the forward-backward asymmetry, depend only on a few specific linear combinations of these operators. The $t\bar{t}$ production by gluon fusion only depends on the coefficient of the operator \mathcal{O}_{hg} . Moreover, only two kinds of four-fermion operators actually contribute to the differential cross section after averaging over the final state spins. The total cross section depends thus only on the three parameters c_{hg} , $c_{Vv} = c_{tq}/2 + (c_{tu} + c_{td})/4 + c_{Qq}^{(8,1)}/2 + (c_{Qu} + c_{Qd})/4$ and $c'_{Vv} = (c_{tu} - c_{td})/2 + (c_{Qu} - c_{Qd})/2 + c_{Qq}^{(8,3)}$.

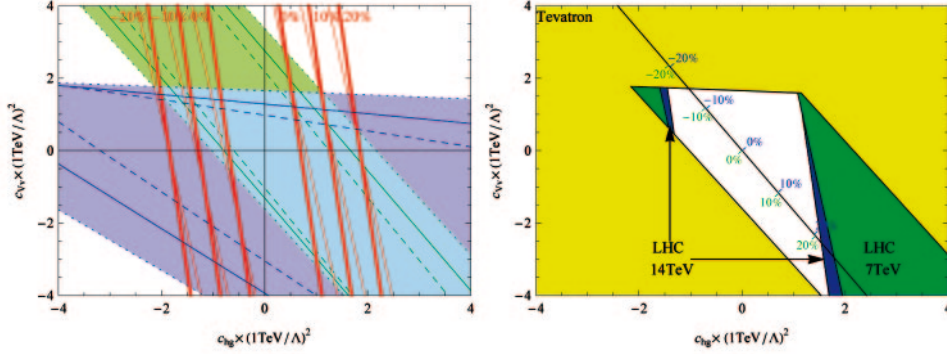


Fig. 4. – (Color online) Left: region allowed by the Tevatron constraints (at 2σ) for $c'_{Vv} = 0$. The green region is allowed by the total cross section measurement. The blue region is consistent with the $t\bar{t}$ invariant mass shape. The red lines show the limits that can be set by the LHC at 7 TeV (thin line) and at 14 TeV (thick line) as soon as a precision on the top pair cross section of 10% and 20% respectively is reached. The “0%” line delimits the region where the new physics contributions are smaller than the theoretical error on the SM cross section. The dashed ($\mu_F = \mu_R = \frac{m_t}{2}$), dotted ($\mu_F = \mu_R = 2m_t$) and solid lines ($\mu_F = \mu_R = m_t = 174.3$ GeV) show the estimated theoretical uncertainties. Right: summary plot (taking $\mu_F = \mu_R = m_t$). The yellow region is excluded by the Tevatron. The green (blue) region is excluded by LHC at 7 TeV (14 TeV) after a precision of 10% is reached on the $t\bar{t}$ cross section (measured to be the SM value).

Numerically, the contribution from the isospin-1 sector (c'_{Vv}) is suppressed compared to the contribution of the isospin-0 sector (c_{Vv}) and this suppression is more effective at the LHC than at the Tevatron. This is due to the fact that at Tevatron, the top pair production by up-quark annihilation is 5–6 times bigger than by down-quark annihilation. At the LHC, this ratio is reduced to 1.4 only. In fig. 4, we take $c'_{Vv} = 0$.

Since top pairs are mainly produced by gluon fusion at the LHC, the measurement of the $t\bar{t}$ cross section at the LHC determines the allowed range for c_{hg} . In contrast, the Tevatron cross section is also sensitive to the four-fermion operators and constrains a combination of c_{hg} and c_{Vv} . The shape of the invariant mass distribution at the Tevatron is sensitive to a combination of c_{Vv} and c_{hg} which is different from the combination controlling the total cross section. It depends quite strongly on the presence of four-fermion operators and is used to further reduce the parameter space mainly along the c_{Vv} direction. Consequently, the measurements of the total cross section at the Tevatron and at the LHC are complementary and combining the two pins down the allowed region in the (c_{hg}, c_{Vv}) plane. We emphasize that the \mathcal{O}_{hg} operator can only be generated at the loop-level in resonance models. Consequently, c_{hg} is expected to be small in such models. Moreover, the new physics and the SM contributions for gluon fusion having a common factor which is mainly responsible for the shape of the distributions of the SM, the operator \mathcal{O}_{hg} can hardly be distinguished from the SM in gluon fusion. Figure 4 summarizes the complementarity between Tevatron and the LHC in constraining the parameter space. Finally, the forward-backward asymmetry A_{FB} probes different operators than those affecting the cross section or the invariant mass distribution:

$$\delta A_{FB}^{\text{dim } 6} = (0.0342^{+0.016}_{-0.009} c_{Aa} + 0.0128^{+0.0064}_{-0.0036} c'_{Aa}) \times \left(\frac{1 \text{ TeV}}{\Lambda} \right)^2,$$

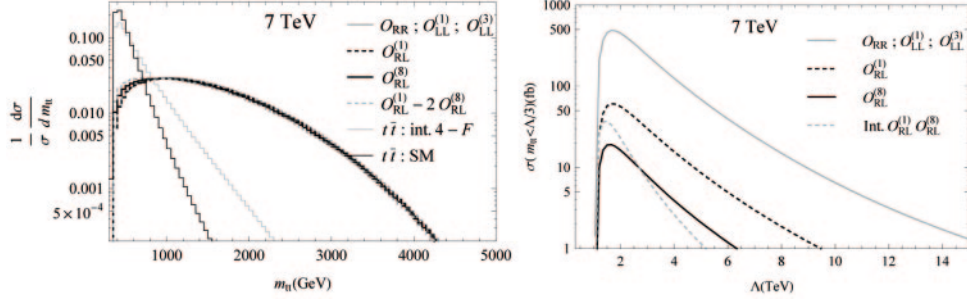


Fig. 5. – Left: normalized invariant mass distribution for tt production at the LHC. The distribution can be trusted only for $m_{tt} \ll \Lambda$. The interference between the SM and the four-fermion operators as well as the SM for $t\bar{t}$ production are also displayed for comparison. Right: cross section of $pp \rightarrow tt$ at the LHC with an upper cut on the invariant mass at $\frac{\Lambda}{3}$ for $c_i = 1$.

where $c_{Aa} = -c_{tq}/2 + (c_{tu} + c_{td})/4 + c_{Qq}^{(8,1)}/2 - (c_{Qu} + c_{Qd})/4$ and $c'_{Aa} = (c_{tu} - c_{td})/2 - (c_{Qu} - c_{Qd})/2 + c_{Qq}^{(8,3)}$. Implications for resonance models are discussed in [12].

The three observables σ , $d\sigma/dm_{t\bar{t}}$ and A_{FB} are unable to disentangle between theories coupled mainly to right- or left-handed top quarks. However, spin correlations allow us to determine which chiralities of the top quark couple to new physics, and in the case of composite models, whether one or two chiralities of the top quark are composite. Spin-dependent observables depend on $c_{Av} = c_{Rv} - c_{Lv}$ and $c'_{Av} = (c_{tu} - c_{td})/2 - (c_{Qu} - c_{Qd})/2 - c_{Qq}^{(8,3)}$. Predictions for deviations at Tevatron and LHC are presented in [11].

3. – Effective field theory for same sign top quark pair production

Like-sign top pair production is a golden channel for early discovery at the LHC as the SM contribution $uu \rightarrow tt$ is absent at tree level. The operators contributing to same sign top pair production are [12]

$$\begin{aligned} \mathcal{O}_{RR} &= [\bar{t}_R \gamma^\mu u_R] [\bar{t}_R \gamma_\mu u_R], \\ \mathcal{O}_{LL}^{(1)} &= [\bar{Q}_L \gamma^\mu q_L] [\bar{Q}_L \gamma_\mu q_L], & \mathcal{O}_{LL}^{(3)} &= [\bar{Q}_L \gamma^\mu \sigma^a q_L] [\bar{Q}_L \gamma_\mu \sigma^a q_L], \\ \mathcal{O}_{LR}^{(1)} &= [\bar{Q}_L \gamma^\mu q_L] [\bar{t}_R \gamma_\mu u_R], & \mathcal{O}_{LR}^{(8)} &= [\bar{Q}_L \gamma^\mu T^A q_L] [\bar{t}_R \gamma_\mu T^A u_R]. \end{aligned}$$

The linear combination $c_{LL} = c_{LL}^{(1)} + c_{LL}^{(3)}$ is severely constrained by B_d mixing [13] to be $|c_{LL}|(\frac{1\text{TeV}}{\Lambda})^2 < 2.1 \times 10^{-4}$ and cannot play any role at the TeV scale. At the partonic level, the leading order differential cross-section for tt production is

$$(1) \quad \frac{d\sigma}{dt} = \frac{1}{\Lambda^4} \left[(|c_{RR}|^2 + |c_{LL}|^2) \frac{(s - 2m_t^2)}{3\pi s} + \left(|c_{LR}^{(1)}|^2 + \frac{2}{9} |c_{LR}^{(8)}|^2 \right) \times \frac{(m_t^2 - t)^2 + (m_t^2 - u)^2}{16\pi s^2} - \left(|c_{LR}^{(1)}|^2 + \frac{8}{3} \Re(c_{LR}^{(1)} c_{LR}^{(8)*}) - \frac{2}{9} |c_{LR}^{(8)}|^2 \right) \frac{m_t^2}{24\pi s} \right].$$

The dominant contribution to this cross section is due to the new physics amplitudes squared because the one-loop SM process is strongly suppressed by $|V_{ub}|^2$ and by the bot-

tom quark mass. Lowest order contributions are thus $\mathcal{O}(\Lambda^{-4})$ contrary to $t\bar{t}$ production for which the largest corrections arise from the $\mathcal{O}(\Lambda^{-2})$ interference. After integration over t , the cross section grows like s as expected from dimensional analysis. In fact, only the interference between the LR operators is proportional to m_t^2 , see eq. (1), and does not have this behaviour. As a consequence, a large part of the total cross section at the LHC comes from the region where $m_{tt} \sim 1$ TeV as shown in fig. 5. In this region, however, the $1/\Lambda$ expansion cannot be trusted for values of Λ around 1 TeV we consider in our study. It therefore does not make sense to express the total cross section at the LHC. There is no such concern at the Tevatron as the m_{tt} distribution is peaked instead below 500 GeV. Figure 5 also displays the cross section with an upper cut on m_{tt} at $\Lambda/3$ as a function of Λ for $c_i = 1$, where c_i is a generic label for the coefficients in eq. (1). This choice ensures that the m_{tt} distribution is at most about 20% below (above) its true value for an s - (t -) channel exchange. The general case can be easily inferred since the coefficient dependences factorise in eq. (1). At 14 TeV, the cross section increases by a factor 2 for $\Lambda \sim 2$ TeV up to a factor 4 for $\Lambda \sim 14$ TeV. Figure 5 shows that the m_{tt} shapes given by the different operators, appear to be quite similar. The maximal effect of the interference term corresponds approximatively to the linear combination $\mathcal{O}_{LR}^{(1)} - 2\mathcal{O}_{LR}^{(8)}$. As foreseen, the interference can only give a sizeable effect for low m_{tt} since it does not grow with s . Again, there are no significant changes at 14 TeV. The distribution is only stretched to the higher invariant mass region.

In contrast with the m_{tt} distribution, the spin correlations provide in principle a very efficient observable to discriminate among the contributions from the various operators in eq. (1). The main reason is that the latter have a well defined chirality structure and no interference with the Standard Model is possible. Strong spin correlations could be used to enhance the sensitivity to the signal and to identify the possible contributing operators. More details can be found in [12] where the (absence of) relation between opposite and same sign top pair productions at the LHC is also discussed. In any case, the LHC has definitely the potential to constrain the corresponding operators.

REFERENCES

- [1] CONTINO R., arXiv:1005.4269 [hep-ph].
- [2] CONTINO R., DA ROLD L. and POMAROL A., *Phys. Rev. D*, **75** (2007) 055014 [hep-ph/0612048].
- [3] PANICO G. and WULZER A., *JHEP*, **09** (2011) 135 [arXiv:1106.2719 [hep-ph]].
- [4] DE CURTIS S., REDI M. and TESI A., arXiv:1110.1613 [hep-ph].
- [5] CONTINO R. and SERVANT G., *JHEP*, **06** (2008) 026 [arXiv:0801.1679 [hep-ph]].
- [6] MRAZEK J. and WULZER A., *Phys. Rev. D*, **81** (2010) 075006 [arXiv:0909.3977 [hep-ph]].
- [7] DISSERTORI G., FURLAN E., MOORTGAT F. and NEF P., *JHEP*, **09** (2010) 019 [arXiv:1005.4414 [hep-ph]].
- [8] CMS- PAS EXO-11-036.
- [9] BINI C., CONTINO R. and VIGNAROLI N., arXiv:1110.6058 [hep-ph].
- [10] BARCELO R., CARMONA A., CHALA M., MASIP M. and SANTIAGO J., *Nucl. Phys. B*, **857** (2012) 172 [arXiv:1110.5914 [hep-ph]].
- [11] DEGRANDE C., GERARD J.-M., GROJEAN C., MALTONI F. and SERVANT G., *JHEP*, **03** (2011) 125 [arXiv:1010.6304 [hep-ph]].
- [12] DEGRANDE C., GERARD J.-M., GROJEAN C., MALTONI F. and SERVANT G., *Phys. Lett. B*, **703** (2011) 306 [arXiv:1104.1798 [hep-ph]].
- [13] BONA M. *et al.* (UTFIT COLLABORATION), *JHEP*, **03** (2008) 049 [arXiv:0707.0636 [hep-ph]].